August 27-31, 2023
FLORENCE - ITALY
ICWE 16
16th International Conference on Wind Engineering

Urban morphology promoting high breathability and controlling strong winds at the pedestrian level

Akashi Mochida[1], Yota Ono[2], Yasuyuki Ishida[3], Ryutaro Ogihara[4]

[1]*Graduate School of Eng., Tohoku University, Sendai, Japan, akashi.mochida.d1@tohoku.ac.jp*
[2]*Graduate School of Eng., Tohoku University, Sendai, Japan, yota.ono.p5@dc.tohoku.ac.jp*
[3]*Graduate School of Eng., Tohoku University, Sendai, Japan, yasuyuki.ishida.e1@tohoku.ac.jp*
[4]*Shimizu Corporation, Tokyo, Japan, r.ogihara@shimz.co.jp*

SUMMARY
Focusing on the reduction in strong winds due to high-rise buildings, many studies have been conducted over the past 50 years in Japan, making it one of the major themes in the field of wind engineering. On the other hand, studies to improve urban ventilation to counter the hot weather in urban areas during summer have been conducted for nearly 20 years. However, hardly any study has simultaneously evaluated the influence of urban morphology on the reduction of strong winds and improvement of ventilation in the urban areas. In this study, large-eddy simulations were performed for nine cases, including urban blocks with a single high-rise building protruding from the surrounding buildings and urban blocks with non-uniform building heights in the whole urban area. In the urban blocks with a single high-rise building, improvements in urban ventilation were observed; however, strong winds occurred at the pedestrian level. In contrast, urban ventilation was improved in urban blocks with non-uniform building heights, and the occurrence of strong winds was suppressed.

Keywords: Breathability, Strong wind, High-rise building, non-uniformity of building heights, LES

1. INTRODUCTION

The reduction in strong winds due to high-rise buildings is a major theme in the field of wind engineering. Considerable knowledge related to the countermeasures against strong winds has been accumulated over the past 50 years in Japan (Murakami et al., 1979; Xu et al., 2017). On the other hand, nearly for the last 20 years, the improvement of ventilation performance within urban areas has been attracting attention as a countermeasure to the urban heat island phenomenon, and many researchers have been studying the improvement of wind velocity at the pedestrian level (Kubota et al., 2008; Yoshie et al., 2008; Ikegaya et al., 2017; Wang et al., 2017) and breathability in urban areas. Breathability, which describes the vertical mixing of air near the ground and air above an urban area (Neophytou et al., 2005), has been evaluated based on air flow rate and vertical momentum flux; it has recently been analyzed by evaluating the vertical kinetic energy flux (Ishida et al., 2018). When considering ways to improve urban ventilation, care should be taken to ensure that excessively strong winds do not occur at the pedestrian level. However, hardly any study has simultaneously evaluated the aspects of strong wind suppression and urban ventilation improvement. This paper presents the results of large-eddy simulations (LESs) evaluating the influence of urban morphology on the breathability of urban areas, mean wind velocity, and strong winds at the pedestrian level.

2. EVALUATION INDICES USED IN THIS STUDY

The mean wind velocity at the pedestrian level was evaluated using the effective speed V_{es} (Eq. (1), Kikumoto et al., 2018), and breathability was evaluated based on the vertical exchange of kinetic energy KE_{ex} at the evaluation height; KE_{ex} comprises the sum of the absolute values of the vertical upward kinetic energy transport E_{+v} and downward transport E_{-v} (Eq. (2)); E_v (Eq. (3)) comprises the mean kinetic energy K transported by advection (first term on the right side) and turbulent diffusion (second term), as well as the turbulent kinetic energy k transported by advection (third term) and turbulent diffusion (fourth term). Strong winds were evaluated by the 95th percentile value of the wind velocity V_{95}, which is the value with a 95% frequency of occurrence from the minimum. The variables used in this study are listed in NOTE 1.

$$V_{es} = \sqrt{\langle(\langle\overline{u_i}\rangle + \overline{u_i}')^2\rangle} = \sqrt{2K + 2k} \quad (1) \qquad KE_{ex} = \int |E_{-v}|dS + \int |E_{+v}|dS \quad (2)$$

$$E_v = \langle\overline{u_i}\,\overline{u_i}\,\overline{u_3}\rangle/2 = \langle\overline{u_3}\rangle K + \langle\overline{u_3}\rangle k + \langle\overline{u_i}'\overline{u_3}'\rangle\langle\overline{u_i}\rangle + \langle\overline{u_i}'\overline{u_3}'\overline{u_i}'\rangle/2 \quad (3)$$

3. ANALYSIS OVERVIEW (NOTE 2

LESs were conducted for the urban areas with a high-rise building taller than the surroundings and with non-uniformity of building heights in the entire urban area, where previous studies reported increased wind speeds at the pedestrian level. The simulation cases included eight types of staggered arrays of simplified building blocks with a plan area index of 25%, and one real urban district in Sendai, Japan (Table 1 and Fig. 1). The inflow was generated using the method proposed by Okaze et al. (2017) (Fig. 2). A run-up calculation was performed over $t^* = 80$ [−] ($= t \times \langle u_{15H}\rangle/H$), and the turbulent statistics were collected and averaged over $t^* = 200$ [−]. Here, $\langle u_{15H}\rangle$ is the time-averaged wind velocity of the inflow at the boundary layer height ($15H$), and H is the building height in Case 1 (= 30 m). All quantities were normalized to H and $\langle u_{15H}\rangle$.

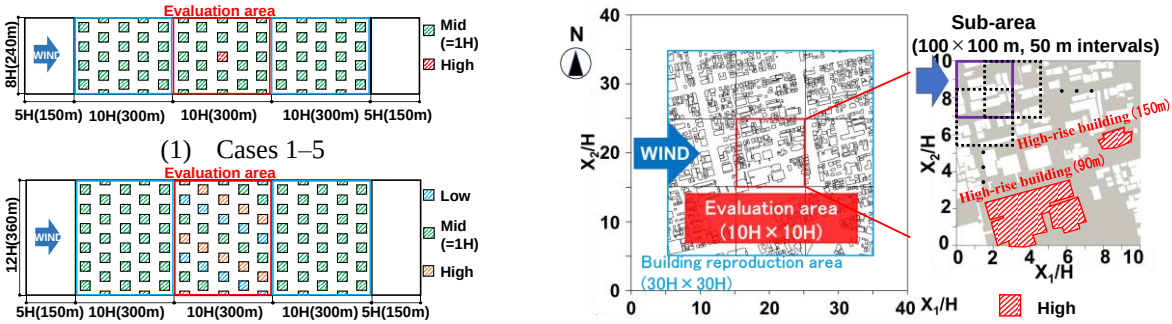

Figure 1. Computational domain and evaluation area (horizontal section)

Table 1. Computed cases

Case	Building Height	σ/H_{ave}
Case 1	1H (uniform)	0
Case 2	1H and 2H (High-rise building)	0.21
Case 3	1H and 3H (High-rise building)	0.40
Case 4	1H and 5H (High-rise building)	0.73
Case 5	1H and 7H (High-rise building)	1.01
Case 6	0.75H, 1H, and 1.25H	0.20
Case 7	0.5H, 1H, and 1.5H	0.41
Case 8	0.25H, 1H, and 1.75H	0.61
Case 9	Average building height: 17.03 m, Standard deviation: 16.95 m	1.00

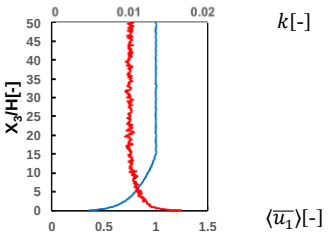

Figure 2. Vertical profiles of inflow conditions

4. RESULTS

In this abstract, the results for Case 5 (case with a single high-rise building), Case 8 (case with non-uniformity), and Case 9 (real urban district) are presented. Fig. 3 shows the distributions of V_{es} and V_{95} at the pedestrian level, and Fig. 4 shows KE_{ex} at the average building height (vertically downward direction is positive). As shown in Figs. 3 (1)–(3), high-rise buildings generated regions with very high values of V_{95} and KE_{ex} only around them. For Case 8, all results were high in the entire area. For Case 9, relatively high-wind-velocity regions were generated from the windward corner of two high-rise buildings on the leeward side. As shown in Fig. 4 depicting KE_{ex}, downward transport can be observed from the windward side of the high-rise building to its side. This value is particularly large for Case 5. Additionally, a correlation between the horizontally averaged KE_{ex} and V_{es} values was confirmed for all the cases. Fig. 5 shows the relationship between the horizontally averaged components of KE_{ex} and maximum V_{95} in the evaluation area. For the cases with a single high-rise building surrounded by buildings with constant height (Cases 2–5), the higher the building height, the larger KE_{ex} and V_{95}. In contrast, in the cases with non-uniform heights (Cases 6–8), as the standard deviation of building height increased, KE_{ex} improved; however, the increase in V_{95} was lower than that in Cases 2–5. It was found that the term with the highest contribution was $\langle\overline{u_3}\rangle K$ (●) in the cases with a single high-rise building and $\langle\overline{u_i}'\overline{u_3}'\rangle\langle\overline{u_i}\rangle$ (▲) in the cases with non-uniform building heights.

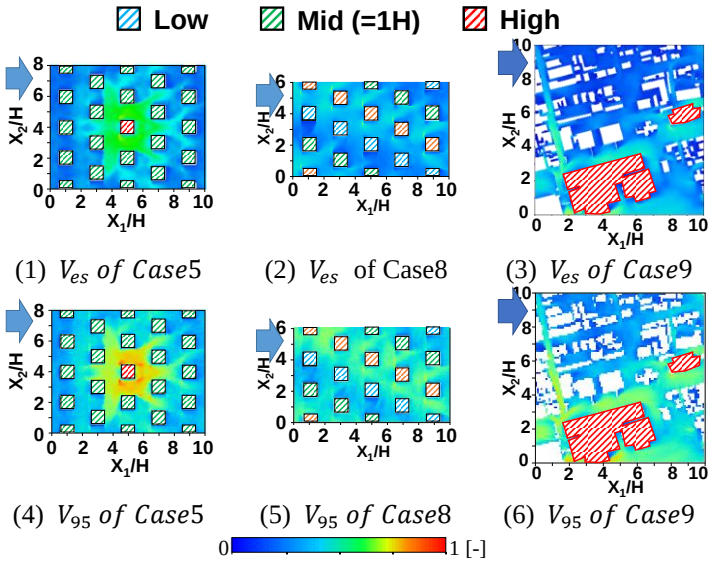

Figure 3. Horizontal distributions of V_{es} and V_{95} at pedestrian height

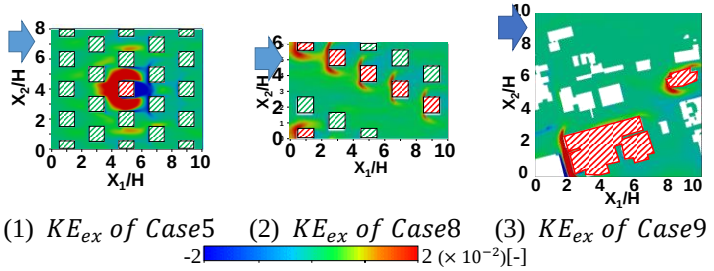

Figure 4. Horizontal distributions of breathability and KE_{ex} at the average building height

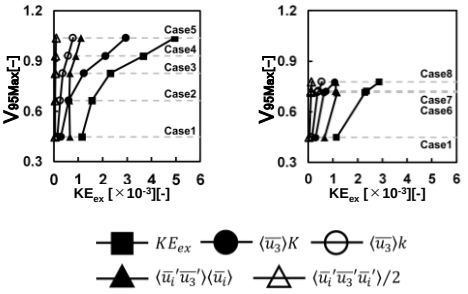

Figure 5. Relationship between KE_{ex} and V_{95}

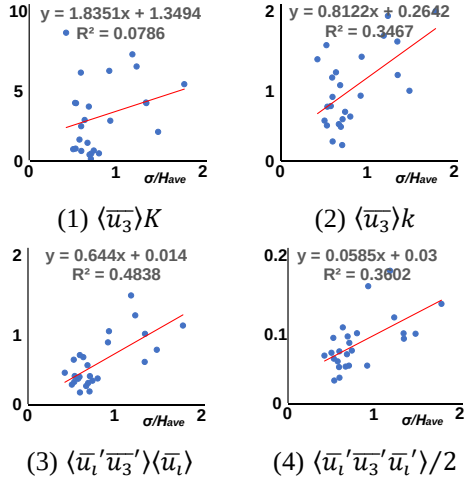

Figure 6. Relationship between standard deviation (σ/H_{ave}) and each component of KE_{ex}(×10^{-3}[-])

Fig. 6 shows the relationship between the standard deviation of building height and each component of KE_{ex} in each sub-area indicated in Fig. 1, with 100-m square sub-areas set at 50-m intervals in Case 9 (real urban district) evaluation area, allowing partial overlap of the neighboring area. The correlation of the standard deviation with K transported by advection was low, whereas its correlations with K and k transported by turbulent diffusion were relatively high. In the case of the real urban district, it was confirmed that transport by turbulent diffusion increased with the standard deviation of the building height.

5. CONCLUSIONS

High-rise buildings that are taller than the surrounding buildings not only increased breathability but also generated a high-wind-speed area around them. However, in the urban area with non-uniform building heights, the breathability by turbulent diffusion was improved, and the occurrence of strong winds was suppressed.

ACKNOWLEDGEMENTS

This research was supported by JSPS KAKENHI, grant number 21H01486.

REFERENCES

Murakami, S., Uehara, K., and Komine, H., 1979. Amplification of wind speed at ground level due to construction of high-rise building in urban area. Journal of Wind Engineering and Industrial Aerodynamics 4, 343-370.

Xu, X., Yang, Q., Yoshida, A., and Tamura, Y., 2017.Characteristics of pedestrian-level wind around super-tall buildings with various configurations. Journal of Wind Engineering and Industrial Aerodynamics 166, 61-73.

Kubota, T., Miura M., Tominaga Y., and Mochida A., 2008. Wind tunnel tests on the relationship between building density and pedestrian-level wind velocity: Development of guidelines for realizing acceptable wind environment in residential neighborhoods, Build. Environ. 43 (10) ,1699-1708.

Yoshie R., Tanaka H., Shirasawa T., and Kobayashi T., 2008. Experimental study on air ventilation in a built-up area with closely-packed high-rise buildings, J. Environ. Eng. (Transactions AIJ) 73, 661-667.

Ikegaya N., Ikeda Y., Hagishima A., Razak A.A., and Tanimoto J., 2017. A prediction model for wind speed ratios at pedestrian level with simplified urban canopies, Theor. Appl. Climatol. 127, 655-665.

Wang W., Ng E., Yuan C., and Raasch S., 2017. Large-eddy simulations of ventilation for thermal comfort - A parametric study of generic urban configurations with perpendicular approaching winds, Urban Clim. 20, 202-227.

Neophytou M.K.-A., and Britter R.E., 2005. Modelling of atmospheric dispersion in complex urban topographies: a computational fluid dynamics study of the central London area, 5th GRACM Int. Congr. Comput. Mech. 2, p. 9

Ishida Y., Okaze T., and Mochida A., 2018. Influence of urban configuration on the structure of kinetic energy transport and the energy dissipation rate, Journal of Wind Engineering & Industrial Aerodynamics 183, 198-213

Kikumoto H., Ooka R., Han M., and Nakajima K., 2018. Consistency of mean wind speed in pedestrian wind environment analyses: Mathematical consideration and a case study using large-eddy simulation. Journal of Wind Engineering & Industrial Aerodynamics, 173, pp.91-99.

Okaze T. and Mochida A, 2017.Cholesky decomposition–based generation of artificial inflow turbulence including scalar fluctuation, Computers & Fluids, 159, pp. 23-32.

NOTES

1. u_i : three components of the instantaneous wind velocity vector (i = 1, 2, 3 for stream-wise, lateral, and vertical directions), $<u_i>$: time-averaged wind velocity vector, u_i' : deviation from time average ($=u_i-<u_i>$), $\overline{u}_i$: filtered variables u_i, K : mean kinetic energy [m^2/s^2] ($=1/2\times\langle\overline{u}_i\rangle^2$), k : turbulent kinetic energy [m^2/s^2] ($=1/2\times\langle\overline{u}_i'\rangle^2$)
2. Code used is OpenFOAM-ver4.1. Grid system was a collocation grid. Time difference scheme was second-order implicit. Advection term scheme was a mixed scheme of 95% second-order central difference and 5% first-order upwind difference in Case1 to Case8, and second-order central difference and 5% first-order upwind difference in Case9. Diffusion term scheme was second-order central difference. PISO method was used for the pressure solution. Boundary conditions of the streamwise direction and top wall were slip. Spalding law was used for the building wall and ground boundary condition. Advection-type boundary condition was used for the outflow boundary.